

UDC 550.8+550.84.09

## SEPARATION OF MAGNETIC ANOMALIES USING FRACTAL METHOD IN THE ESFORDI REGION FOR IRON EXPLORATION, CENTRAL EAST IRAN

**Amin Karimi Kalvarzi**<sup>1</sup>,  
Aref.shirazi@aut.ac.ir

**Aref Shirazi**<sup>1</sup>,  
Aref.shirazi@aut.ac.ir

**Adel Shirazy**<sup>1</sup>,  
Adel.shirazy@shahroodut.ac.ir

**Amin Beiranvand Pour**<sup>2</sup>,  
beiranvand.pour@umt.edu.my

**Ardehshir Hezarkhani**<sup>1</sup>,  
Ardehez@aut.ac.ir

**Hamed Nazerian**<sup>1</sup>,  
hamed.nazerian@studium.unict.it

**Timofey V. Timkin**<sup>3</sup>,  
timkin@tpu.ru

**Valery G. Voroshilov**<sup>3</sup>,  
v\_g\_v@tpu.ru

<sup>1</sup> Amirkabir University of Technology (Tehran Polytechnic),  
Hafez avenue, 1591634311, Tehran, Iran.

<sup>2</sup> University Malaysia Terengganu (UMT),  
Kuala Nerus, 21030, Terengganu, Malaysia.

<sup>3</sup> National Research Tomsk Polytechnic University,  
30, Lenin avenue, Tomsk, 634050, Russia.

**The relevance** of the research is determined by the possibilities of measuring the potential magnetic field, which has self-similar (fractal) properties, as well as a practical tool for prospecting and exploration of iron ores. In the Esfordi area, this method was used by us for the first time to identify, separate and interpret geophysical (magnetic) anomalies.

**The main aim** of this thematic and practical study is the qualitative interpretation of geophysical data, the application of new methods in the prospecting and exploration of mineral deposits, modeling the geological environment and forecasting new promising areas.

**Object:** Esfordi region, Yazd province, Iran.

**Methods.** To obtain additional information about the subsurface, magnetometric data were used with their interpretation by the RTP (reduction to the north magnetic pole) method. For modeling purposes, an artificial sample was made, consisting of a sphere, a cube and a cuboid, and it was found that the fractal method can be used to separate anomalies for unipolar models (cube and cuboid).

**Results.** The results of the study were applied to the Esfordi region, where it was found that at a survey scale of 1:100000, there is a direct relationship between the fractal method and the 3D model, which can be used to locate iron ore mineralization.

### **Key words:**

magnetic anomalies, fractal, RTP-area method, modeling, iron ores, Esfordi region, Iran.

### **Introduction**

In today's complex world, where we are witnessing advances in various technologies, especially in the mining industry, new methods and technologies in estimating the depth of anomalies during mineral exploration seem necessary [1–11]. Studies on iron ores have also been carried out in abundance in various formats [12–17], because iron is widely used in various industries such as automotive, electronics, etc. [18, 19]. To better advance, magnetic phenomena must be studied. Isolation of magnetic anomalies from the field and then an accurate determination of its model is one of the most critical parameters extracted from geophysical data interpretation [20–24]. One of the experimental methods that emerged with the advancement of technology and science was the experimental geophysical method. As its name implies, the experimental geophysical methods deal with the physics of the earth and the surrounding atmosphere. These methods are used to determine underground reserves and resources such as reservoirs of hydrocarbons and metal minerals, physical properties of the earth's layers, separate the earth's layers, and the location of geological structures. The methods used in geophysical

exploration are based on physical principles. Magnetic exploration is one of the oldest geophysical exploration methods that has been used for many years in mineral exploration and economic mineralogy, and even for archaeological purposes. This method also identifies magnetic sources between sedimentary layers such as deep igneous or volcanic intrusions. In mineral exploration, the magneto metric method is very effective for exploring both magnetic and non-magnetic minerals associated with magnetic minerals. Sedimentary rocks usually have minor magnetic effects, so changes in the intensity of the magnetic field at the earth's surface are mostly related to lithological changes in basement rocks or igneous intrusions. Minimal changes in the concentration of magnetite during the diagenesis process cause minimal anomalies. Various computational methods are widely used in data processing, an essential part of anomaly analysis. In this section, methods are used to help separate specific anomalous components. The measured magnetic field follows the principle of inhibition of anomalies from different sources. These principles are: (1) Remaining anomalies located in the study area; (2) Deep and significant geological resources

create regional components with long wave-lengths; (3) Low wavelength components created due to tracking errors and observation of shallow and small information and sources.

One of the steps in the final interpretation is removing the disturbing regional components and noises in the anomalous field from the remaining field. This principle is solved based on separating the remaining anomalies by eliminating or weakening the regional anomalies and noise [3, 4]. An important goal in interpreting potential field data is to improve the resolution of observed data. In magnetic exploration, in areas where there is a limited outcrop, by determining the lateral changes of magnetic susceptibility, information can be obtained not only about the lithological changes but also about the structural process of the area [23–26]. In potential field analysis, many algorithms are designed to extract shallow information [3, 27–29]. The method of anomaly separation from the field can be divided into two groups, which include structural (based on the spatial distribution of data) and non-structural (based on the structural distribution of data) [5, 29–33]. Classical statistics assumed that statistical parameters would lead to a normal distribution or normal log in previous years. This assumption emphasizes the frequency distribution of parameters, but spatial variability, particularly spatial correlation information, is ignored [34–37]. The difference between structural and non-structural methods is that structural methods generalize the coordinates of points and their positions. Generally, an anomaly with a small amount in the field can reduce the overall anomaly. Non-structural methods can be useful to solve some problems according to the distribution and spatial position of the sample [38], for example, we can refer to the grade-area model in the fractal method [39]. The concept of fractals to describe the modeling and analysis of complex phenomena, processes of self-testing, or scale immutability was described by Mandelbrot [40]. In the last 40 years, the concept of fractal has expanded significantly from geo-metric sets to multidimensional contexts [2, 31, 41]. In recent years, the fractal method has been introduced in earth sciences, physics, chemistry, medicine and mineral processing and has become a popular scientific topic in the scientific community [42].

So far, many algorithms have been devised to separate the anomaly from the context, in other words, to identify boundaries with different characteristics of the context. In general, the main concerns in the diagnosis of anomalies can be expressed in two cases: (1) How to identify the field; and (2) Determining the possibility of an irregular border.

Fractal and multi-fractal models are used to quantify patterns such as geophysical data. Fractal and multi-fractal modeling is widely used to differentiate various mineralization [5, 16, 17]. This method has several limitations, especially when boundary effects are involved in irregular geometric data sets [18]. The primary method used for all cases seems to be the concentration-area method, which means that geophysical distributions mainly satisfy the properties of a fractal function. There is evidence that geophysical and

geochemical data distribution has fractal behavior in nature [19, 20]. This theory develops an alternative interpretation validation and improves proper methods for the analysis of geophysical distributions.

Before using statistical methods on actual data, they are usually tested on artificial data to confirm their effect. Due to the complexity of artificial calculations, magnetic sources often replace simple geometric shapes (spheres, prisms, or cubes) that are very representative of natural geological sources [43]. Therefore, in this paper, to express the effect of the cut-area model in the fractal method on accurate data, we apply this method to an artificial sample consisting of three simple geometric shapes.

#### Research methodology

The Fractals result from the self-similarity of parameters associated with scale instability and refer to the property of a system that does not change with scale change. Mandelbrot introduces fractals to describe patterns composed of parts with a geometry (shape) and are more or less similar to the general pattern regardless of scale [44, 45]. There are different models for distributing the fractal method, including number-size model [46], concentration-area model [47–50] and concentration-distance model [34]. Due to the complexity of magnetic field issues, a variety of maps have been developed by experts over the years, each of which contains some form of exploratory information. In the polarization map (RTP), due to the transfer of the anomalous location to the magnetic pole, where the earth's magnetic field becomes vertical, the effect of the geographical location of the harvest site, i. e. the angles of inclination and deflection, is eliminated. This processing causes the location of the magnetic anomaly to be corrected relative to the site of the mineralization, and in fact, the magnetic anomaly is placed on top of the deposit. Due to the nature of magnetic field vectoring and the variation in inclination angle and deflection angle concerning the magnetic equator, maximum magnetic anomalies are transmitted directly from the sources, and the anomalies are very asymmetric. This complicates the interpretation of anomalies, especially at lower latitudes [3]. Therefore, to counter this effect, Baranov proposed a method for converting magnetic anomalies at any magnetic latitude to anomalies based on the sheer magnetism and the vertical field based on the Poisson relation [22].

One of the methods based on fractal distribution is the concentration-area one. This method, proposed by Cheng and his colleagues, is based on an area that occupies a unique scale in the study area [39]. Instead of the term concentration, the term pole reversal is used in this research, and the RTP-area model, i. e. specific areas that occupy the polarized reversal levels in the study area, is investigated.

The general formula of the model proposed by Cheng and his colleagues is defined according by the equation (1):

$$A(\rho \leq \nu)\alpha\rho^{-\alpha_1}; A(\rho \geq \nu)\alpha\rho^{-\alpha_2}, \quad (1)$$

where  $\rho$  is equal to the RTP plane and  $A(\rho)$  is the area of the regions with  $\rho$  plane;  $v$  is the threshold values;  $\alpha_1$  and  $\alpha_2$  are the fractal dimensions [34, 44, 51–53].

This method has advantages over similar cases in classical statistics:

- (1) independence of data in the RTP-area fractal method;
- (2) consideration of the geological situation in data distribution;
- (3) independence of standard or non-normal data.

This method considers the exact spatial position of the samples to separate the anomaly from the background. In addition, there is no need to delete out-of-line data in this method because the fractal nature of the data automatically removes these items [44, 45, 54, 55].

To obtain the enclosed area, the contour map of the desired area should be prepared using software such as Surfer, Geosoft, or GIS to calculate the area of each level line [56–63]. After drawing the contour map of the data for each cell, a value is specified that represents its RTP, and each cell has its unique area. The levels are arranged in ascending order, and for each repetitive level, only one item is recorded along with its total areas in the table. After performing the calculations, the whole logarithmic diagram of the RTP area is drawn. An exponential

relationship should be observed in the diagram. The threshold values are obtained from the breakpoints in the last step, and the anomaly map is drawn based on the threshold values [30, 41, 64, 65].

#### Artificial Data

A synthetic prototype was produced by Model vision 13.0 software [47, 66, 67]. In this example, three simple geometric sources of a sphere, rectangular cube and square cube, were used. The parameters used and the coordinates of the midpoints of these three sources are shown in Table. The deflection angle and magnetic inclinations were 50 and 3 degrees, respectively, and the magnetic field strength was selected in the modeling range of 47000 nT. Fig. 1, *a* shows a three-dimensional view of the artificial specimen.

Artificial data were generated on this model with 10 in 10 networking. According to the artificial data, a general magnetic field map was created for this sample. The general magnetic field map became the pole reversal map because it does not accurately show the exact position of the magnetic field on the ground [43, 52, 68–74]; Fig. 1, *b* shows the RTP map.

**Table.** Geometric parameters of the three sources used

**Таблица.** Геометрические параметры трех используемых источников

Number Число	Source Источник	Midpoint coordinates/meter Координаты средней точки/метр	Length/Длина			Magnetic resistance Магнитное сопротивление
			X/meter X/метр	Y/meter Y/метр	Z/meter Z/метр	
1	Sphere/Сфера	(143.1,880.7,300)	60	60	60	0,03
2	Cuboid/Кубоид	(596.9,773.4,200)	60	380	75	0,02
3	Cube/Куб	(190.1,614.9,250)	150	150	150	0,03

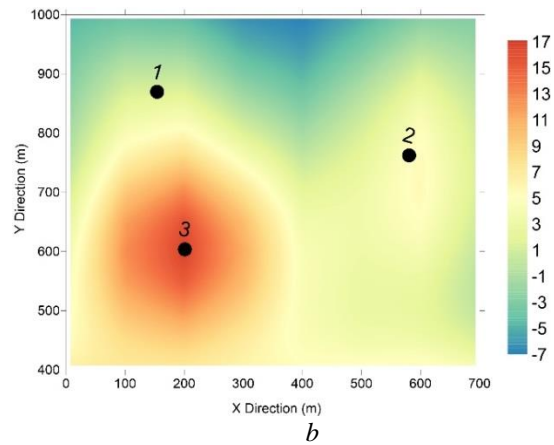
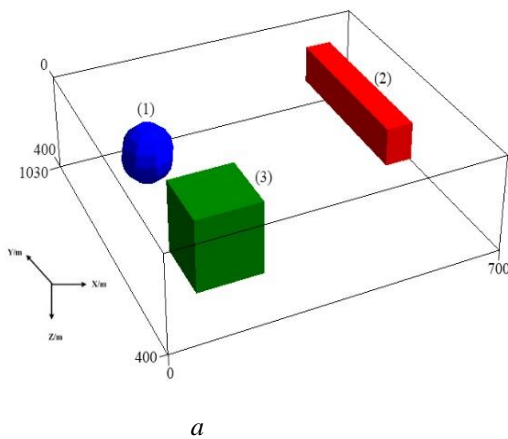


**Fig. 1.** Three-dimensional view of the sources used in the artificial model (*a*) and reversal map to the pole of the artificial model (*b*)

**Рис. 1.** Трехмерный вид источников, используемых в искусственной модели (*a*), и карта разворота к полюсу искусственной модели (*b*)

For the fractal model, we obtain the area of the levels in Fig. 1, *b*. The distance of each level in this sample was set to 0,1. Fig. 2, *a* shows an all-logarithmic RTP-area diagram for artificial data. According to the thresholds obtained from this diagram, the anomaly is separated from the field in Fig. 2, *b*. As can be seen, the desired anomaly for the square-cube source is well represented, while for the rectangular cube source, there is little

separation. Due to this anomaly in the interpretation of the spherical source is placed between the positive and negative poles. In the whole logarithmic diagram, negative data is removed, the RTP-area method alone cannot separate the boundaries of such layers. However, it is possible that in the areas where the boundaries of the layers are most prominent, they are somewhat close to the source of the square cube.

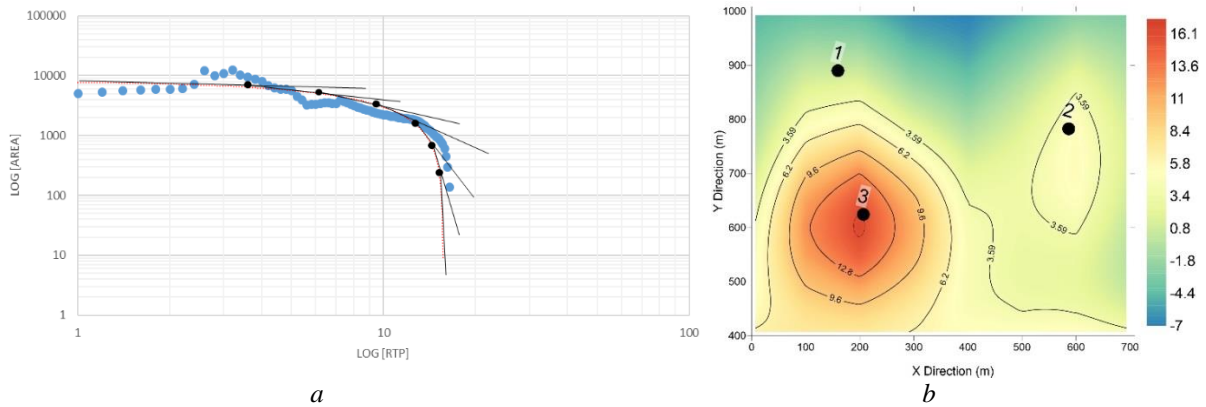


**Fig. 2.** Full logarithmic diagram of RTP-area (a) and anomaly separation map from the field on artificial data (b)  
**Рис. 2.** Полная логарифмическая диаграмма RTP-области (a) и карта разделения аномалий от поля по искусственным данным (b)

**Case study**

The study area is located on 1:100000 Esfordi in the south of Yazd province. This area is located 15 km east of Bafgh city and 14 km southwest of the Bafgh iron mine (Fig. 3). Geologically, this area contains dolomite, shale, sandstone along with tuff and acidic lavas (Fig. 4).

Iron ore is formed in the bulk, lens, and layered form in Upper Precambrian deposits, and its main minerals are magnetite, ilmenite, hematite, and to a lesser extent, pyrite. Gang apatite is present in relatively large amounts in this ore. Esfordi iron ore, black spot, Mishdovan, and Narigan ores are the most critical views of this deposit.

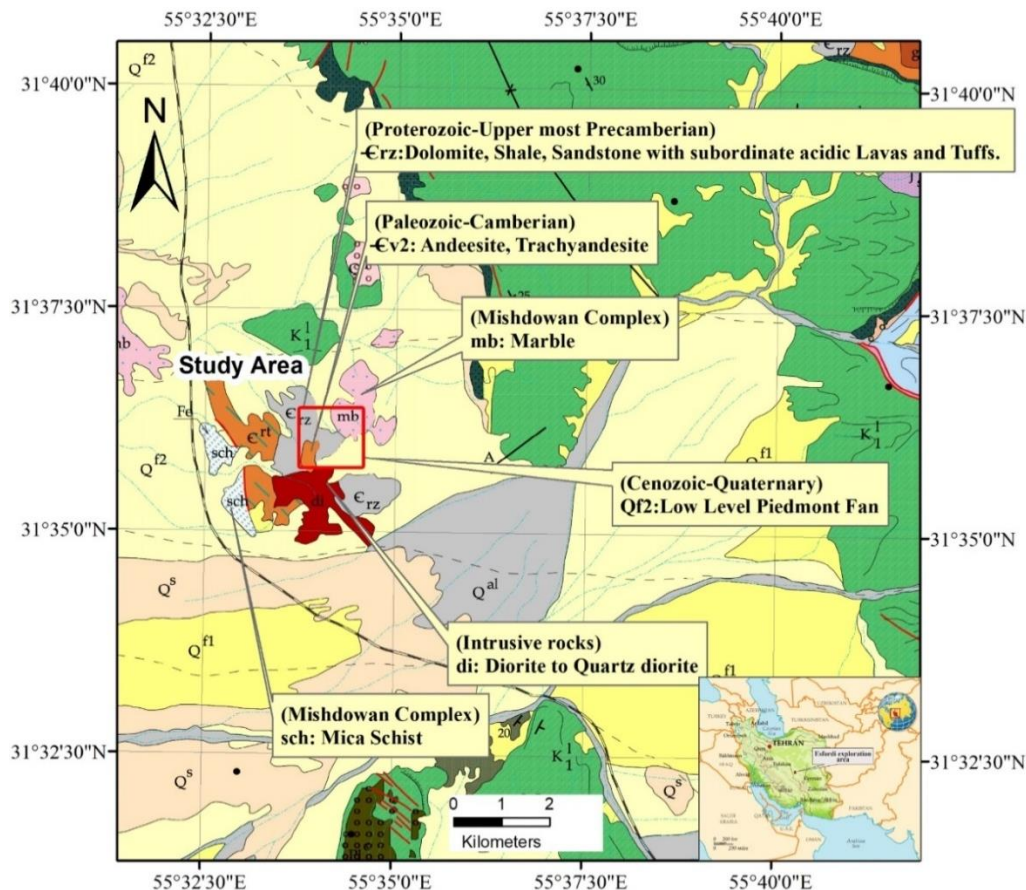


**Fig. 3.** Schematic geological map of the Esfordi exploration area in Central East Iran  
**Рис. 3.** Схематическая геологическая карта разведочного района Эсфорди в центрально-восточном Иране

The area in which the magnetometric survey has been carried out has an extension of about 1,5 km in the east-west direction and 1,7 km in the north-south direction. In order to interpret the magnetic data in the study area,

1320 points with a distance of 40 meters from the stations and 20 meters from the profiles have been taken from each other. After making the necessary corrections to the data, a map of the whole magnetic field for the desired

range was prepared (Fig. 4, a). The changes in this field result from the Earth's magnetic field and local fields due to the presence of a magnetic source in the range. In this map, two anomalies are observed, one of which is in a bipolar zone with an east-west trend.

Furthermore, another anomaly is in the center of the range, the negative pole of which is widely around and very irregular. It is important to note that the two anomalies, due to their small distance, affect the measurement of the related magnetic field. The nature of the anomalies is bipolar, and since the angle of inclination and magnetic deflection of the Earth is a function of the geographical location of the measuring points, therefore,

the shape of the source, in addition to magnetic susceptibility, depends on the magnetic induction of the Earth. This phenomenon is one of the factors complicating the analysis of magnetic maps. To solve this problem, a polarizing filter is used. In this case, the anomalies are located vertically above the source. As mentioned before, a pole in the desired range is prepared to show the exact position of the anomalies on the map. To prepare the reversal map to the pole in the deflection angle and magnetic inclination range, 49 and 3,3 degrees were applied on the whole magnetic field map, respectively. Fig. 4, b shows the reversal map to the pole of this range.

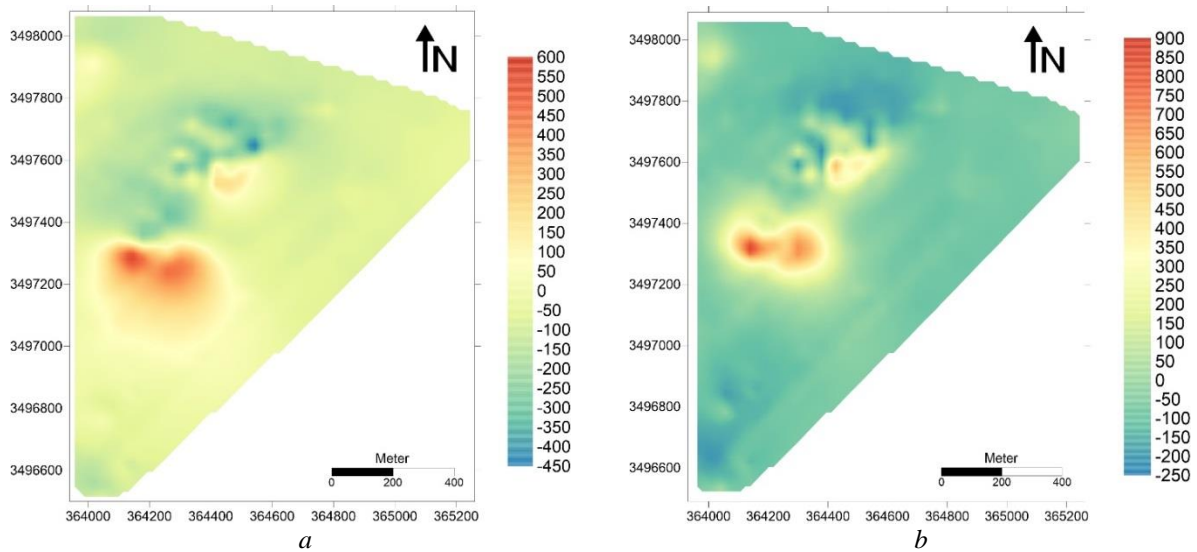


**Fig. 4.** Map of the total magnetic field (a) and map of return to the pole (b)  
**Рис. 4.** Карта полного магнитного поля (a) и карта разворота к полюсу (b)

The distance of the levels of the reversal map to the pole nT 1 was considered, and the area of each level was calculated. The complete logarithmic diagram of the

RTP-area was plotted according to Fig. 5, a. According to Fig. 5, b, the anomaly is isolated from the field according to the thresholds obtained from Fig. 5, a.

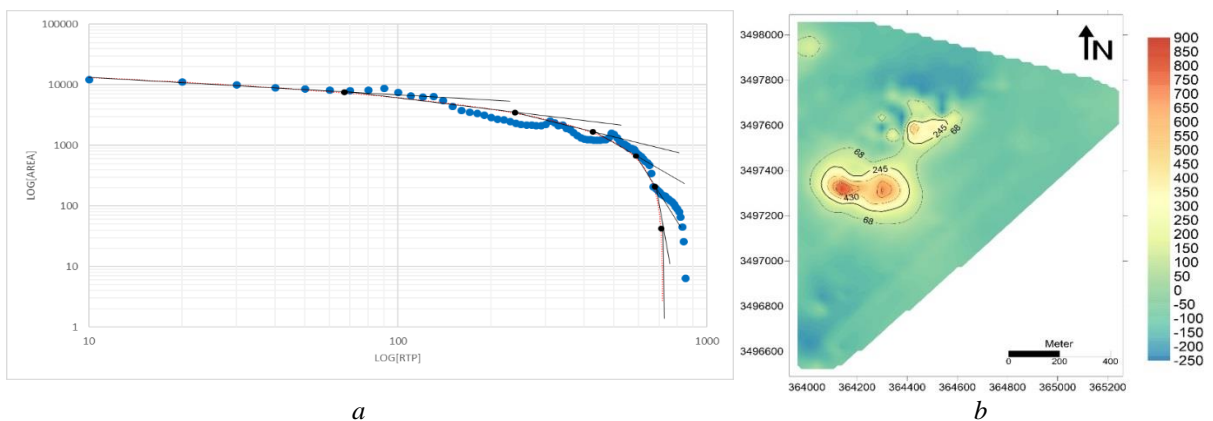


**Fig. 5.** Full logarithmic diagram of RTP-area (a) and anomaly separation map from the background for the study area (b)  
**Рис. 5.** Полная логарифмическая диаграмма RTP-района (a) и карта отделения аномалий от фона для изучаемой территории (b)

To obtain the depth of anomalies, the area in which the three anomalies are located was separated, and the depth was estimated. Then, depth estimates were performed for structural indicators and different window sizes, and the

results were displayed on the polarization map (Fig. 6). After the examinations, a suitable structural index of 1 and a suitable window size of 15×15 were found. This diagnosis is estimated after various surveys on the map. It

means that with different studies, this diagnosis does not contain out-of-row values and all points are on the trend of abnormalities. According to the anomaly results, A is a sloping dyke which western part is less deep than its

eastern part, which indicates that the source has a slope to the east. This anomaly in the western part of the depth is about  $10 \pm 40$  meters. The depths of anomalies B and C are also approximately 40 meters.

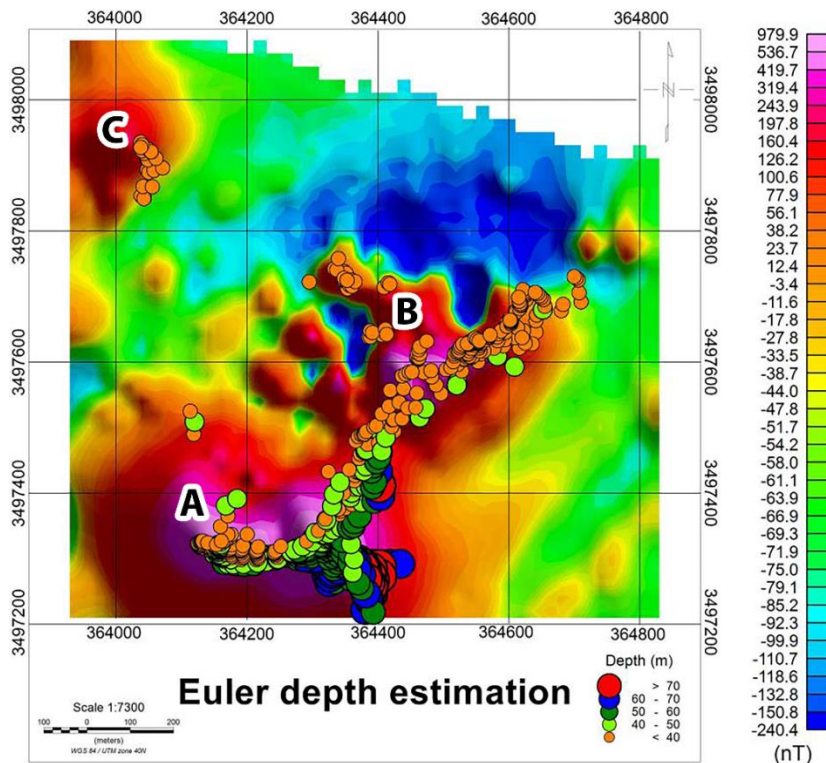


Fig. 6. Estimation of the study area depth

Рис. 6. Карта с оценкой глубины изучаемой области

Since most field studies have an inherent complexity, performing two-dimensional modeling for exploration purposes does not seem sufficient, and the need for three-dimensional modeling is well felt. Leading modeling is one of the valuable methods for modeling. Because the model parameters can be part of a proportional inverse procedure, different model parameters are created for modeling. Most of the leading models in the potential field are based on simple integral equations that can represent the magnetic distribution of the source in a polygon [43]. After estimating the approximate position and depth of the magnetic field anomaly using the residual field analysis and estimating the depth, it is possible to model the magnetic source three-dimensionally (magnetic anomaly generating mass).

The mathematical process of predicting data based on some physical or mathematical model is a specific set of model parameters, available information, and source geometry. We create an artificial model and use it to generate predicted data. One of the critical parameters for performing advanced modeling is the correct estimation of the magnetic self-susceptibility of the anomalous generating mass. The most important aspect of modeling is the simulation of horizontal gradients, which can be observed by calculating and comparing the observed horizontal derivatives and modeling them. The amplitude of the modeled anomaly can be compared by adjusting the adaptation of the magnetic contrast properties in the final stage.

In magnetometric impressions, the total composition of the magnetic field is usually measured on a horizontal plane. The purpose of the impressions is to determine the magnetization distribution of the source, estimate the depth of the source, and the direction of magnetization of the entire source. According to the uncertainty principle in field answers, the interpretive potential has difficulty achieving the above answers, and this uncertainty is induced in theoretical models. According to this principle, countless theoretical models can create similar magnetic anomalies. Minimizing the number of answers in modeling requires all available geophysical and geological information. For example, field sampling and determining the magnetic self-susceptibility of samples in the laboratory can be one way to reduce uncertainty. It should also be noted that surface samples are not closely related to deeper samples.

Reducing the effect of this principle on modeling results is possible in three ways: mathematics, geophysics, and geology. The geophysical magnetization determined by reverse modeling should not be much different from the values measured in the laboratory. From a geological point of view, it is necessary to observe the relationship between the anomaly pattern and its generative structure so that the chosen model is selected correctly at the beginning of the simulation.

To compare the results of the fractal method discussed in this paper, a three-dimensional simulation of the range was performed according to the Lee–Oldenburg method.

Using this method, the variable on which the interpretation will be based is first decided, magnetic self-acceptance or magnetic self-acceptance logarithm or a function of magnetic self-acceptance. A multi-component objective function is then constructed with sufficient flexibility to produce various models. The form of this objective function is such that it can be corrected for acceptable mathematical undesirable aspects such as the concentration of magnetic self-acceptance near the surface, the substantial structure, or the presence of negative magnetic self-acceptance. This objective function compensates for unevenness in three spatial directions and weighs based on the distribution of profound magnetic susceptibility. Three-dimensional auxiliary weighting functions in the objective function can combine more information about the model [23]. Such information may be available from other geophysical excavations, geological data, or the interpreter's quantitative and qualitative understanding of the geological structure and its relationship to magnetic susceptibility. These three-dimensional weighting functions can also be used to the answer questions about the magnetic susceptibility properties found in previous inverters. In this approach, negative magnetic

susceptibility is neglected by constructing a transformation of variables and solving a nonlinear reversal problem. Numerical solutions for inversion by dividing the earth into large cells have been realized to make relatively complex geological objects.

In this modeling, Mag3D software based on the Lee–Oldenburg method was used. The final source model is determined by preparing the data, entering them into the software environment, and determining the required parameters. For the study area, the dimensions of the mesh were determined according to the area's dimensions (length and width of the area), the length and width of the mesh were 16 meters, and its height was 8 meters. Then the magnitude of magnetic self-susceptibility to the separation of the anomaly from the field values was considered equal to 0,1 in the SI unit. The final model is shown in Fig. 7. As can be seen in this figure, the two sources of anomalies A and B in the range are identified, confirming the previous breadth and depth results. The source of the C anomaly is probably not present in the results of this modeling because it did not have a good scope in design. The maximum depth of the anomalies has continued up to about 700 meters, which is unrealistic because the accuracy of this method is low at great depths.

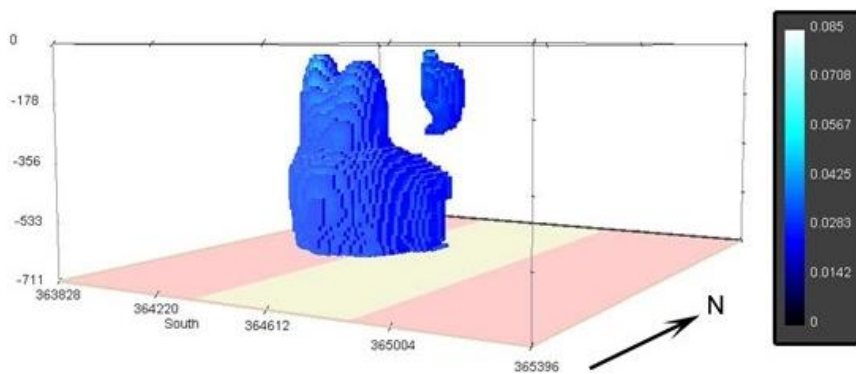


Fig. 7. Model obtained from the sources of the study area using the Lee–Oldenburg method

Рис. 7. Модель, полученная из источников исследуемой территории по методу Ли–Ольденбурга

Fig. 8, a shows a section of a three-dimensional diagram of the magnetic susceptibility data of the target area. To illustrate the point, Fig. 8, b shows the data

having magnetic self-susceptibility between 0,07 and 0,08. It can be seen that the existing masses have a source almost similar to the square-cube model.

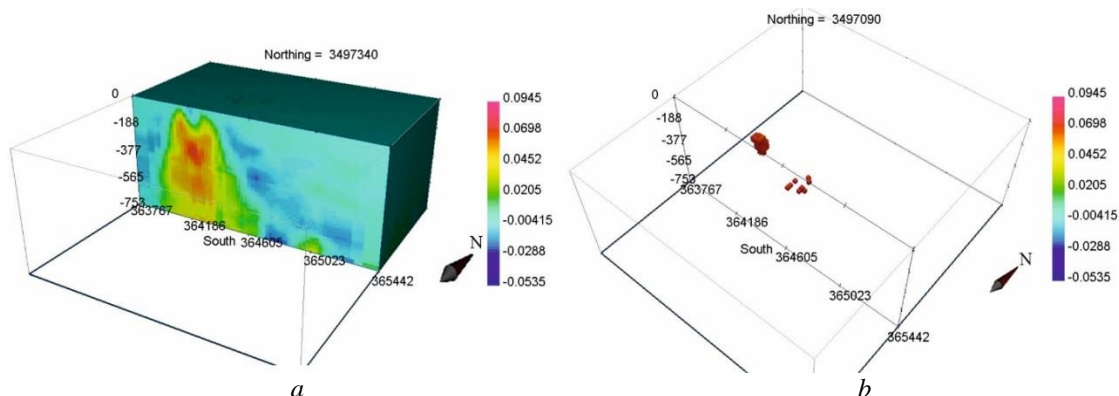


Fig. 8. Three-dimensional form of the magnetic self-susceptibility of the study area (a) and sources with magnetic susceptibility (b)

Рис. 8. Трехмерная форма геофизической аномалии исследуемой области (a) и возможные источники с магнитной восприимчивостью (b)

### Discussion and conclusions

According to the studies performed in the maps of the total magnetic field and the rest of the magnetic field, three anomalies in the range are clear and visible. Different maps are being discussed that failed to pinpoint the source of the anomaly. It is because the negative pole of the magnetic anomaly is not clear. The polarization map also confirms the possibility of a bipolar one for anomalies. While in the quasi-gravitational map this hypothesis can be refuted to some extent.

In this paper, the fractal is used to isolate magnetic anomalies from the field. Due to the superiority of this method over classical statistical methods, the RTP-area method was used for this purpose. Considering that artificial modeling is necessary to have more information for fractal calculations on accurate data, an artificial sample containing three types of sources was created. The results show that the sources of the square-cube have a relative proportion to the fractal models in the anomalous separation from the field. Considering that the spherical source has created two positive and negative poles in this sample, it can be seen that this method has some shortcomings in separating the anomalies between these two poles. The isolated data in the case study show that sources with a structure similar to the square-cube model

can be separated by the RTP-area fractal method. It is necessary to use this method for sources with a small depth, and the separation of magnetic anomalies from the field at great depths without considering specific parameters cannot be cited.

This study aimed to explore the source of iron ore and to isolate magnetic anomalies from the field. The identified area can be exploratory prioritized for further geochemical and geophysical studies. Due to the peculiarities of the geology of the region, in addition to magnetite, hematite also has the potential for mineralization in this area, which can be investigated by other geophysical methods (gravimetric, seismological and electrical) for a more detailed study. Because weak magnetic anomalies have been reported with high prevalence, it is recommended that at least the range gravimetric be taken. The possible source could be the mineralization of magnetite, which has been converted to hematite in the surface parts.

*This paper has been produced benefiting from the 2232 International Fellowship for Outstanding Researchers Program of TÜBİTAK (Project No: 118C219). However, the entire responsibility of the paper belongs to the owner of the paper. The financial support received from TÜBİTAK does not mean that the content of the publication is approved in a scientific sense by TÜBİTAK.*

### REFERENCES

1. Shirazy A., Shirazy A., Nazerian H. Application of remote sensing in earth sciences – a review. *International Journal of Science and Engineering Applications*, 2021, vol. 10, pp. 45–51.
2. Gupta A.K., Srivastava S. Delineation of sulfide mineralization over a part of western margin of greenstone belt of the Dhanjori Basin, Singhbhum Craton from petrophysical, petrographic and geophysical studies. *Precambrian Research*, 2022, vol. 368, pp. 1–20.
3. Kaftan I. Interpretation of magnetic anomalies using a genetic algorithm. *Acta Geophysica*, 2017, vol. 65, no. 4, pp. 627–634.
4. Shirazy A., Ziaii M., Hezarkhani A., Timkin T. Geostatistical and remote sensing studies to identify high metallogenic potential regions in the Kivi area of Iran. *Minerals*, 2020, vol. 10, pp. 1–25.
5. Wang G., Zhang S., Yan C., Xu G., Ma M., Li K., Feng Y. Application of the multifractal singular value decomposition for delineating geophysical anomalies associated with molybdenum occurrences in the Luanchuan ore field (China). *Journal of Applied Geophysics*, 2012, vol. 86, pp. 109–119.
6. Timkin T., Abedini M., Ziaii M., Ghasemi M.R. Geochemical and hydrothermal alteration patterns of the Abrisham-Rud Porphyry Copper District, Semnan Province, Iran. *Minerals*, 2022, vol. 12, no. 1, pp. 1–24.
7. Ben U.C., Akpan A.E., Urang J.G., Akaerue E.I., Obianwu V.I. Novel methodology for the geophysical interpretation of magnetic anomalies due to simple geometrical bodies using social spider optimization (SSO) algorithm. *Heliyon*, 2022, vol. 8, no. 3, pp. 1–21.
8. Shirazy A., Hezarkhani A., Shirazy A., Timkin T.V., Voroshilov V.G. Geophysical explorations by resistivity and induced polarization methods for the copper deposit, South Khorasan, Iran. *Bulletin of the Tomsk Polytechnic University. Geo Assets Engineering*, 2022, vol. 333, no. 3, pp. 99–110. In Rus.
9. Cherkasova (Yakich) T., Kucherenko I., Abramova R. Rear polymetamorphic zone of near-veined metasomatic aureole in mesothermal Zun-Holba golddeposit (Eastern Sayan). *IOP Conference Series: Earth and Environmental Science*, 2015, vol. 27, pp. 1–5.
10. Timkin T., Voroshilov V., Askanakova O., Cherkasova T., Chernyshov A., Korotchenko T. Estimating gold-ore mineralization potential within Topolninsk ore field (Gorny Altai). *IOP Conference Series: Earth and Environmental Science*, 2015, vol. 27, pp. 1–5.
11. Yakich T.Y., Ananyev Y.S., Ruban A.S., Gavrilov R.Y., Lesnyak D.V., Levochkaia D.V., Savinova O.V., Rudmin M.A. Mineralogy of the Svetloye epithermal district, Okhotsk-Chukotka volcanic belt, and its insights for exploration. *Ore Geol. Rev.*, 2021, vol. 136, 104257.
12. Shirazy A., Hezarkhani A., Timkin T., Shirazi A. Investigation of magneto-/radio-metric behavior in order to identify an estimator model using K-means clustering and Artificial Neural Network (ANN) (Iron Ore Deposit, Yazd, Iran). *Minerals*, 2021, vol. 11, no. 12, pp. 1–18.
13. Sheykhi V., Moore F. Evaluation of potentially toxic metals pollution in the sediments of the Kor River, southwest Iran. *Environmental monitoring and assessment*, 2013, vol. 185, no. 4, pp. 3219–3232.
14. Eslamizadeh A. Geological setting of iron oxide-apatite deposits in the Bafq district, central Iran with an emphasis on mineralogical, petrographic, and geochemical study of the Sechahun deposit. *Iranian Journal of Earth Sciences. Iranian Journal of Earth Sciences*, 2016, vol. 8, no. 2, pp. 147–163.
15. Majidi S., lotfi M., Emami M.H., Nezafati N. Investigation on the genesis of the iron oxide-apatite=REE deposits of the Bafgh-Saghand district (Central Iran), based on oxygen isotope studies. *Journal of Geoscience*, 2018, vol. 28, no. 109, pp. 237–244.
16. Pagano G., Aliberti F., Guida M., Oral R., Siciliano A., Trifuoggi M., Tommasi F. Rare earth elements in human and animal health: state of art and research priorities. *Environmental research*, 2015, vol. 142, pp. 215–220.
17. Wang G., Carranza E.J.M., Zuo R., Hao Y., Du Y., Pang Z., Sun Y., Qu J. Mapping of district-scale potential targets using fractal models. *Journal of Geochemical Exploration*, 2012, vol. 122, pp. 34–46.
18. Liang T., Li K., Wang L. State of rare earth elements in different environmental components in mining areas of China. *Environmental monitoring and assessment*, 2014, vol. 186, no. 3, pp. 1499–1513.
19. Carranza E.J.M. Catchment basin modelling of stream sediment anomalies revisited: incorporation of EDA and fractal analysis. *Geochemistry: Exploration, Environment, Analysis*, 2010, vol. 10, pp. 365–381.
20. Nazerian E., Gharebaghi S., Safdarian A. Optimal distribution network reconfiguration considering power quality issues. *Smart Grid Conference (SGC)*, 2017, pp. 1–6.



21. Nazerian E., Tahami F. Optimum design of planar transformer for LLC resonant converter using metaheuristic method. *IECON 2019 – 45th Annual Conference of the IEEE Industrial Electronics Society*. Lisbon, Portugal, 2019. pp. 6621–6626.
22. Khayer K., Shirazy A., Shirazi A., Ansari A., Nazerian H., Hezarkhani A. Determination of Archie's Tortuosity factor from Stoneley waves in carbonate reservoirs. *International Journal of Science and Engineering Applications*, 2021, vol. 10, no. 08, pp. 107–110.
23. Shirazy A., Shirazi A., Nazerian H., Khayer K., Hezarkhani A. Geophysical study: estimation of deposit depth using gravimetric data and Euler method (Jalalabad iron mine, kerman province of IRAN). *Open Journal of Geology*, 2021, vol. 1, pp. 340–355.
24. Shirazy A., Shirazi A., Ferdossi M.H., Ziai M. Geochemical and geostatistical studies for estimating gold grade in tarq prospect area by k-means clustering method. *Open Journal of Geology*, 2019, vol. 9, no. 6, pp. 306–326.
25. Pignatelli A., Nicolosi I., Chiappini M. An alternative 3D inversion method for magnetic anomalies with depth resolution. *Annals of Geophysics*, 2006, vol. 49, no. 4–5, pp. 1021–1027.
26. Shirazy A., Ziai M., Hezarkhani A., Timkin T.V., Voroshilov V.G. Geochemical behavior investigation based on K-means and artificial neural network prediction for titanium and zinc, Kivi region, Iran. *Bulletin of the Tomsk Polytechnic University. Geo Assets Engineering*, 2021, vol. 332, no. 3, pp. 113–125. In Rus.
27. Oruç B., Selim H. Interpretation of magnetic data in the Sinop area of Mid Black Sea, Turkey, using tilt derivative, Euler deconvolution, and discrete wavelet transform. *Journal of Applied Geophysics*, 2011, vol. 74, no. 4, pp. 194–204.
28. Alahgholi S., Shirazy A., Shirazi A. Geostatistical studies and anomalous elements detection, Bardaskan Area, Iran. *Open Journal of Geology*, 2018, vol. 8, no. 7, pp. 697–710.
29. Shirazi A., Shirazy A., Saki S., Hezarkhani, A. Geostatistics studies and geochemical modeling based on core data, Sheytoor Iron Deposit, Iran. *Journal of Geological Resource and Engineering*, 2018, vol. 6, pp. 124–133.
30. Mohammadi N.M., Hezarkhani A., Saljooghi B.S. Separation of a geochemical anomaly from background by fractal and U-statistic methods, a case study: Khooni district, Central Iran. *Geochemistry*, 2016, vol. 76, no. 4, pp. 491–499.
31. Shirazi A., Shirazy A., Saki S., Hezarkhani A. Introducing a software for innovative neuro-fuzzy clustering method named NFCMR. *Global Journal of Computer Sciences: theory and research*, 2018, vol. 8, no. 2, pp. 62–69.
32. Shirazi A., Shirazy A. Introducing geotourism attractions in Toroud village, Semnan Province, Iran. *International Journal of Science and Engineering Applications*, 2020, vol. 9, no. 6, pp. 79–86.
33. Timkin T.V., Voroshilov V.G., Yurkova M.V., Mansour Z. Ore mineralogy of Sokhatiny gold deposit (Northeast Asia, Russia). *Bulletin of the Tomsk Polytechnic University. Geo Assets Engineering*, 2022, vol. 333, no. 4, pp. 53–65. In Rus.
34. Li C., Ma T., Shi J. Application of a fractal method relating concentrations and distances for separation of geochemical anomalies from background. *Journal of Geochemical exploration*, 2003, vol. 77, no. 2–3, pp. 167–175.
35. Doodran R.J., Khakmardan S., Shirazi A., Shirazy A. Minimalization of ash from Iranian Gilsonite by Froth Flotation. *Journal of Minerals and Materials Characterization and Engineering*, 2021, vol. 9, pp. 1–13.
36. Shirazi A., Hezarkhani A., Shirazy A. Remote sensing studies for mapping of iron oxide regions, South of Kerman, Iran. *International Journal of Science and Engineering Applications*, 2018, vol. 7, no. 4, pp. 45–51.
37. Shirazi A., Shirazy A., Karami J. Remote sensing to identify copper alterations and promising regions, Sarbishe, South Khorasan, Iran. *International Journal of Geology and Earth Sciences*, 2018, vol. 4, no. 2, pp. 36–52.
38. Grunsky E., Agterberg F. Spatial and multivariate analysis of geochemical data from metavolcanic rocks in the Ben Nevis area, Ontario. *Mathematical Geology*, 1988, vol. 20, no. 7, pp. 825–861.
39. Cheng Q., Agterberg F., Ballantyne S. The separation of geochemical anomalies from background by fractal methods. *Journal of Geochemical exploration*, 1994, vol. 51, no. 2, pp. 109–130.
40. Mandelbrot B. How long is the coast of Britain? Statistical self-similarity and fractional dimension. *Science*, 1967, vol. 3775, no. 156, pp. 636–638.
41. Chen G., Cheng Q., Zhang H. Matched filtering method for separating magnetic anomaly using fractal model. *Computers & Geosciences*, 2016, vol. 90, pp. 179–188.
42. Liu J., Ding W., Dai J., Zhao G., Sun Y., Yang H. Unreliable determination of fractal characteristics using the capacity dimension and a new method for computing the information dimension. *Chaos, Solitons & Fractals*, 2018, vol. 113, pp. 16–24.
43. Pignatelli A., Nicolosi I., Carluccio R., Chiappini M., Von Frese R. Graphical interactive generation of gravity and magnetic fields. *Computers & Geosciences*, 2011, vol. 37, no. 4, pp. 567–572.
44. Mandelbrot B.B., Passoja D.E., Paullay A.J. Fractal character of fracture surfaces of metals. *Nature*, 1984, vol. 308, no. 5961, pp. 721–722.
45. Mandelbrot B.B. *The fractal geometry of nature*. New York, WH freeman, 1982. 460 p.
46. Wang Q.F., Wan L., Zhang Y., Zhao J., Liu H. Number-average size model for geological systems and its application in economic geology. *Nonlinear Processes in Geophysics*, 2011, vol. 18, no. 4, pp. 447–454.
47. Zuo R., Xia Q., Zhang D. A comparison study of the C–A and S–A models with singularity analysis to identify geochemical anomalies in covered areas. *Applied Geochemistry*, 2013, vol. 33, pp. 165–172.
48. Guan W., Hu H., Wang Z. Permeability inversion from low-frequency seismoelectric logs in fluid-saturated porous formations. *Geophysical Prospecting*, 2013, vol. 61, no. 1, pp. 120–133.
49. Panichev A. Rare earth elements: review of medical and biological properties and their abundance in the rock materials and mineralized spring waters in the context of animal and human geophagia reasons evaluation. *Achievements in the Life Sciences*, 2015, vol. 9, no. 2, pp. 95–103.
50. Ahmadi H., Rahmani A.B. Study on the mineral anomalies of Muqur-Chaman fault and its comparison with Harirud (Herat) fault (Afghanistan) using geophysical and remote sensing (Aster-HyMap) data. *Geology and bowels of the earth*, 2018, no. 1 (66), pp. 28–38.
51. Agharezaei M., Hezarkhani A. Delineation of geochemical anomalies based on Cu by the boxplot as an exploratory data analysis (EDA) method and concentration-volume (CV) fractal modeling in Mesgaran mining area, Eastern Iran. *Open Journal of Geology*, 2016, vol. 6, no. 10, pp. 1269–1278.
52. Daigle H., Johnson A., Thomas B. Determining fractal dimension from nuclear magnetic resonance data in rocks with internal magnetic field gradients. *Geophysics*, 2014, vol. 79, no. 6, pp. 425–431.
53. Meakin P. Fractal aggregates in geophysics. *Reviews of Geophysics*, 1991, vol. 29, no. 3, pp. 317–354.
54. Mazzarella A., Tranfaglia G. Fractal characterisation of geophysical measuring networks and its implication for an optimal location of additional stations: an application to a rain-gauge network. *Theoretical and Applied Climatology*, 2000, vol. 65, no. 3, pp. 157–163.
55. Turcotte D.L. Fractals in geology and geophysics. *Pure and applied Geophysics*, 1989, vol. 131, no. 1, pp. 171–196.
56. Ghorbani M. *The economic geology of Iran: mineral deposits and natural resources*. New York, Springer, 2013. 569 p.
57. Lehmann B. Economic geology of rare earth elements in 2014: a global perspective. *European Geologist*, 2014, vol. 37, pp. 21–24.
58. Menard S. *Applied logistic regression analysis*. Sage publications. London, Sage Publications, 2001. 111 p.
59. Guan W., Hu H., Wang Z. Technospheric mining of rare earth elements from bauxite residue (Red Mud): process optimization, kinetic investigation, and microwave pretreatment. *Scientific Reports*, 2017, vol. 7, no. 1, pp. 1–9.
60. Zhang W., Liao G., Qin Q. Based on open-source GIS platform to build 2D visual geophysical information management software. *Geophysical and Geochemical Exploration*, 2014, vol. 5, pp. 1064–1069.
61. Faults J.E. *Geologic map and cross sections of the McGinness Hills Geothermal Area – GIS data*. Las Vegas, University of Nevada, 2013.
62. Pawlowski R. GIS applied to exploration: Caserta Block, Central Apennines, southern Italy. *The Leading Edge*, 2000, vol. 19, no. 2, pp. 193–196.
63. Ekosse G., Fouche P.S. Using GIS to understand the environmental chemistry of manganese contaminated soils,

- Kgwakgwe area, Botswana. *Journal of Applied Sciences and Environmental Management*, 2005, vol. 9, no. 2, pp. 37–42.
64. Shahsavari S., Rad J.A., Afzal P., Nezafati N., Akhavan A.M. Prospecting for polymetallic mineralization using step-wise weight assessment ratio analysis (SWARA) and fractal modeling in Aghkand Area, NW Iran. *Arabian Journal of Geosciences*, 2019, vol. 12, no. 7, pp. 1–10.
65. Yan Z.-H. Seismic random noise attenuation based on empirical mode decomposition of fractal dimension. *Chinese Journal of Geophysics*, 2017, vol. 60, no. 7, pp. 2845–2857.
66. Al-Ghamdi A., Aguilera R., Clarkson C.R. Cementation exponent estimation for complex carbonate reservoirs using a triple porosity model. *Society of Petroleum Engineers - SPE/DGS Saudi Arabia Section Technical Symposium and Exhibition*. Al-Khobar, Saudi Arabia, 2011, pp. 159–170.
67. Jacobson J.J., Yacout A.M., Matthem G.E., Piet S.J., Shropshire D.E., Jeffers R.F., Schweitzer T. Verifiable fuel cycle simulation model (VISION): a tool for analyzing nuclear fuel cycle futures. *Nuclear Technology*, 2010, vol. 172, no. 2, pp. 157–178.
68. MacLeod I.N., Jones K., Dai T.F. 3-D analytic signal in the interpretation of total magnetic field data at low magnetic latitudes. *Exploration geophysics*, 1993, vol. 24, no. 3–4, pp. 679–688.
69. Pulkkinen A., Kuznetsova M., Ridley A., Raeder J., Vapirev A., Weimer D., Weigel R.S., Wiltberger M., Millward G., Rastätter L., Hesse M., Singer H.J., Chulaki A. Geospace environment modeling 2008–2009 challenge: ground magnetic field perturbations. *Space Weather*, 2011, vol. 9, no. 2, pp. 1–13.
70. Fogler M., Koulakov A., Shklovskii B. Ground state of a two-dimensional electron liquid in a weak magnetic field. *Physical Review B*, 1996, vol. 54, no. 3, pp. 1853–1871.
71. Bu Y.Y., Erdmenger J., Shock J.P., Strydom M. Magnetic field induced lattice ground states from holography. *Journal of High Energy Physics*, 2013, vol. 165, pp. 1–28.
72. Ashoori R.C., Stormer H.L., Weiner J.S., Pfeiffer L.N., Baldwin K.W., West K.W. N-electron ground state energies of a quantum dot in magnetic field. *Physical review letters*, 1993, vol. 71, no. 4, pp. 613–616.
73. Gorbar E., Miransky V., Shovkovy I. Normal ground state of dense relativistic matter in a magnetic field. *Physical Review D*, 2011, vol. 83, no. 8, pp. 1–26.
74. Liu P., Liu T., Zhu P., Yang Y., Zhou Q., Zhang H., Chen G. Depth estimation for magnetic/gravity anomaly using model correction. *Pure & Applied Geophysics*, 2017, vol. 174, no. 4, pp. 1729–1742.

Received: 24 September 2022.

Reviewed: 3 March 2023.

#### Information about the authors

- Amin Karimi Kalvarzi**, PhD, assistant, Amirkabir University of Technology (Tehran Polytechnic).  
**Aref Shirazi**, PhD, assistant, Amirkabir University of Technology (Tehran Polytechnic).  
**Adel Shirazy**, PhD, assistant, Amirkabir University of Technology (Tehran Polytechnic).  
**Amin Beiranvand Pour**, PhD, associate professor, University Malaysia Terengganu.  
**Ardeshir Hezarkhani**, PhD, full professor, Amirkabir University of Technology (Tehran Polytechnic).  
**Hamed Nazerian**, PhD, assistant, Amirkabir University of Technology (Tehran Polytechnic).  
**Timofey V. Timkin**, Cand. Sc., associate professor, National Research Tomsk Polytechnic University.  
**Valery G. Voroshilov**, Dr. Sc., professor, National Research Tomsk Polytechnic University.

УДК 550.8+550.84.09

## РАЗДЕЛЕНИЕ МАГНИТНЫХ АНОМАЛИЙ ФРАКТАЛЬНЫМ МЕТОДОМ ДЛЯ ПОИСКА ЖЕЛЕЗНЫХ РУД, РАЙОН ЭСФОРДИ, ЦЕНТРАЛЬНО-ВОСТОЧНЫЙ ИРАН

Амин Карими Калварзи<sup>1</sup>,  
Adel.shirazy@shahroodut.ac.ir

Ареф Ширази<sup>1</sup>,  
Adel.shirazy@shahroodut.ac.ir

Адель Ширази<sup>1</sup>,  
Adel.shirazy@shahroodut.ac.ir

Амин Бейранванд Пур<sup>2</sup>,  
beiranvand.pour@umt.edu.my

Ардешир Хезархани<sup>1</sup>,  
Ardehez@aut.ac.ir

Хамед Назерян<sup>1</sup>,  
Adel.shirazy@shahroodut.ac.ir

Тимкин Тимофей Васильевич<sup>3</sup>,  
timkin@tpu.ru

Ворошилов Валерий Гаврилович<sup>3</sup>,  
v\_g\_v@tpu.ru

<sup>1</sup> Технологический университет им. Амир Кабира (Тегеранский политехнический институт), Иран, 1591634311, Тегеран, Авеню Хафеза.

<sup>2</sup> Университет Малайзии Теренгану, Малайзия, 21030, Теренгану, Куала-Нерус.

<sup>3</sup> Национальный исследовательский Томский политехнический университет, Россия, 634050, г. Томск, пр. Ленина, 30.

**Актуальность** исследований определяется возможностями измерений потенциального магнитного поля, которое обладает самоподобными (фрактальными) свойствами, вследствие чего фрактальный метод можно использовать для выявления магнитных аномалий, а также как практический инструмент для поиска и разведки железных руд. На площади Эсфорди этот метод использован нами впервые для выявления, разделения и интерпретации геофизических (магнитных) аномалий.

**Основной целью** данного тематического и практического исследования является качественная интерпретация геофизических данных, применение новых методов при поисках и разведке месторождений полезных ископаемых, моделировании геологической среды и прогнозировании новых перспективных участков.

**Объект:** район Эсфорди, провинция Йезд, Иран.

**Методы.** Для получения дополнительной информации о недрах использовались магнитометрические данные с интерпретацией их методом RTP (редукция к северному магнитному полюсу). Для целей моделирования был изготовлен искусственный образец, состоящий из сферы, куба и прямоугольного параллелепипеда, и было обнаружено, что фрактальным методом можно провести разделение аномалий для униполярных моделей (куба и прямоугольного параллелепипеда).

**Полученные результаты.** Результаты исследования были применены к региону Эсфорди, где установлено, что в масштабе исследований 1:100000 между фрактальным методом и трехмерной моделью существует прямая связь, которая может быть использована для определения местоположения железорудной минерализации.

### Ключевые слова:

магнитные аномалии, фрактал, метод RTP, моделирование, железные руды, район Эсфорди, Иран.

Статья была подготовлена в рамках Международной стипендиальной программы для выдающихся исследователей TÜBİTAK 2232 (проект № 118C219). Однако вся ответственность за публикацию статьи лежит на её владельце. Финансовая поддержка, полученная от TÜBİTAK, не означает, что содержание публикации одобрено TÜBİTAK в научном смысле.

### СПИСОК ЛИТЕРАТУРЫ

1. Shirazy A., Shirazy A., Nazerian H. Application of remote sensing in earth sciences – a review // International Journal of Science and Engineering Applications. – 2021. – V. 10. – P. 45–51.
2. Gupta A.K., Srivastava S. Delineation of sulfide mineralization over a part of western margin of greenstone belt of the Dhanjori Basin, Singhbhum Craton from petrophysical, petrographic and geophysical studies // Precambrian Research. – 2022. – V. 368. – P. 1–20.
3. Kaftan I. Interpretation of magnetic anomalies using a genetic algorithm // Acta Geophysica. – 2017. – V. 65. – № 4. – P. 627–634.
4. Geostatistical and remote sensing studies to identify high metallogenic potential regions in the Kivi Area of Iran / A. Shirazy, M. Ziaii, A. Hezarkhani, T. Timkin // Minerals. – 2020. – V. 10. – P. 1–25.
5. Application of the multifractal singular value decomposition for delineating geophysical anomalies associated with molybdenum occurrences in the Luanchuan ore field (China) / G. Wang, S. Zhang, C. Yan, G. Xu, M. Ma, K. Li, Y. Feng // Journal of Applied Geophysics. – 2012. – V. 86. – P. 109–119.
6. Geochemical and hydrothermal alteration patterns of the Abrisham-Rud Porphyry Copper District, Semnan Province, Iran / T. Timkin, M. Abedini, M. Ziaii, M.R. Ghasemi // Minerals. – 2022. – V. 12. – № 1. – P. 1–24.
7. Novel methodology for the geophysical interpretation of magnetic anomalies due to simple geometrical bodies using social spider optimization (SSO) algorithm / U.C. Ben, A.E. Akpan, J.G. Urang, E.I. Akaerue, V.I. Obianwu // Heliyon. – 2022. – V. 8. – № 3. – P. 1–21.
8. Применение геофизических методов удельного электрического сопротивления и вызванной поляризации при поиске медных руд, южный Хорасан, Иран / А. Ширази, А. Хезархани, А. Ширази, Т.В. Тимкин, В.Г. Ворошилов // Известия Томского политехнического университета. Инжиниринг георесурсов. – 2022. – Т. 333. – № 3. – С. 99–110.
9. Cherkasova (Yakich) T., Kucherenko I., Abramova R. Rearpolymineral zone of near-veined metasomatic aureole in

- mesothermal Zun-Holba gold deposit (Eastern Sayan) // IOP Conference Series: Earth and Environmental Science. – 2015. – V. 27. – P. 1–5.
10. Estimating gold-ore mineralization potential within Topolninsk ore field (Gorny Altai) / T. Timkin, V. Voroshilov, O. Askanakova, T. Cherkasova, A. Chernyshov, T. Korotchenko // IOP Conference Series: Earth and Environmental Science. – 2015. – V. 27. – P. 1–5.
  11. Mineralogy of the Svetloye epithermal district, Okhotsk-Chukotkavolcanic belt, and its insights for exploration / T.Yu. Yakich, Y.S. Ananyev, A.S. Ruban, R.Y. Gavrilov, D.V. Lesnyak, D.V. Levochkaia, O.V. Savinova, M.A. Rudmin // Ore Geology Reviews. – 2021. – V. 136. – 104257.
  12. Investigation of magneto-radio-metric behavior in order to identify an estimator model using K-means clustering and Artificial Neural Network (ANN) (Iron Ore Deposit, Yazd, IRAN) / A. Shirazy, A. Hezarkhani, T. Timkin, A. Shirazi // Minerals. – 2021. – V. 11. – № 12. – P. 1–18.
  13. Sheykhi V., Moore F. Evaluation of potentially toxic metals pollution in the sediments of the Kor River, southwest Iran // Environmental monitoring and assessment. – 2013. – V. 185. – № 4. – P. 3219–3232.
  14. Eslamizadeh A. Geological setting of iron oxide-apatite deposits in the Bafq district, central Iran with an emphasis on mineralogical, petrographic, and geochemical study of the Sechahun deposit // Iranian Journal of Earth Sciences. Iranian Journal of Earth Sciences. – 2016. – V. 8. – № 2. – P. 147–163.
  15. Investigation on the genesis of the iron oxide-apatite=REE deposits of the Bafgh-Saghand district (Central Iran), based on oxygen isotope studies / S. Majidi, M. lotfi, M.H. Emami, N. Nezafati // Journal of Geoscience. – 2018. – V. 28. – № 109. – P. 237–244.
  16. Rare earth elements in human and animal health: state of art and research priorities / G. Pagano, F. Aliberti, M. Guida, R. Oral, A. Siciliano, M. Trifuoggi, F. Tommasi // Environmental research. – 2015. – V. 142. – P. 215–220.
  17. Mapping of district-scale potential targets using fractal models / G. Wang, E.J.M. Carranza, R. Zuo, Y. Hao, Y. Du, Z. Pang, Y. Sun, J. Qu // Journal of Geochemical Exploration. – 2012. – V. 122. – P. 34–46.
  18. Liang T., Li K., Wang L. State of rare earth elements in different environmental components in mining areas of China // Environmental monitoring and assessment. – 2014. – V. 186. – № 3. – P. 1499–1513.
  19. Carranza E.J.M. Catchment basin modelling of stream sediment anomalies revisited: incorporation of EDA and fractal analysis // Geochemistry: Exploration, Environment, Analysis. – 2010. – V. 10. – P. 365–381.
  20. Nazerian E., Gharebaghi S., Safdarian A. Optimal distribution network reconfiguration considering power quality issues // Smart Grid Conference (SGC). – 2017. – P. 1–6.
  21. Nazerian E., Tahami F. Optimum design of planar transformer for LLC resonant converter using metaheuristic method // IECON 2019 – 45<sup>th</sup> Annual Conference of the IEEE Industrial Electronics Society. – Lisbon, Portugal, 2019. – P. 6621–6626.
  22. Determination of Archie's tortuosity factor from Stoneley waves in carbonate reservoirs / K. Khayer, A. Shirazy, A. Shirazi, A. Ansari, H. Nazerian, A. Hezarkhani // International Journal of Science and Engineering Applications. – 2021. – V. 10. – № 08. – P. 107–110.
  23. Geophysical study: estimation of deposit depth using gravimetric data and Euler method (Jalalabad iron mine, kerman province of IRAN) / A. Shirazy, A. Shirazi, H. Nazerian, K. Khayer, A. Hezarkhani // Open Journal of Geology. – 2021. – V. 1. – P. 340–355.
  24. Geochemical and geostatistical studies for estimating gold grade in tarq prospect area by k-means clustering method / A. Shirazy, A. Shirazi, M.H. Ferdossi, M. Ziaii // Open Journal of Geology. – 2019. – V. 9. – № 6. – P. 306–326.
  25. Pignatelli A., Nicolosi I., Chiappini M. An alternative 3D inversion method for magnetic anomalies with depth resolution // Annals of Geophysics. – 2006. – V. 49. – № 4–5. – P. 1021–1027.
  26. Исследование геохимического поведения титана и цинка на основе метода k-средних и искусственных нейронных сетей для прогнозирования новых площадей, регион Киви, Иран / А. Ширази, М. Зиани, А. Хезархани, Т.В. Тимкин, В.Г. Ворошилов // Известия Томского политехнического университета. Инжиниринг георесурсов. – 2021. – Т. 332. – № 3. – С. 113–125.
  27. Oruç B., Selim H. Interpretation of magnetic data in the Sinop area of Mid Black Sea, Turkey, using tilt derivative, Euler deconvolution, and discrete wavelet transform // Journal of Applied Geophysics. – 2011. – V. 74. – № 4. – P. 194–204.
  28. Alahgholi S., Shirazy A., Shirazi A. Geostatistical studies and anomalous elements detection, Bardaskan Area, Iran // Open Journal of Geology. – 2018. – V. 8. – № 7. – P. 697–710.
  29. Geostatistics studies and geochemical modeling based on core data, Sheytoor iron deposit, Iran / A. Shirazi, A. Shirazy, S. Saki, A. Hezarkhani // Journal of Geological Resource and Engineering. – 2018. – V. 6. – P. 124–133.
  30. Mohammadi N.M., Hezarkhani A., Saljooghi B.S. Separation of a geochemical anomaly from background by fractal and U-statistic methods, a case study: Khooni district, Central Iran // Geochemistry. – 2016. – V. 76. – № 4. – P. 491–499.
  31. Introducing a software for innovative neuro-fuzzy clustering method named NFCMR / A. Shirazi, A. Shirazy, S. Saki, A. Hezarkhani // Global Journal of Computer Sciences: theory and research. – 2018. – V. 8. – № 2. – P. 62–69.
  32. Shirazi A., Shirazy A. Introducing geotourism attractions in Toroud village, Semnan Province, Iran // International Journal of Science and Engineering Applications. – 2020. – V. 9. – № 6. – P. 79–86.
  33. Минералогия руд Сохагинского золоторудного месторождения (Северо-Восток Азии, Россия) / Т.В. Тимкин, В.Г. Ворошилов, М.В. Юркова, М. Зиани // Известия Томского политехнического университета. Инжиниринг георесурсов. – 2022. – Т. 333. – № 4. – С. 53–65.
  34. Li C., Ma T., Shi J. Application of a fractal method relating concentrations and distances for separation of geochemical anomalies from background // Journal of Geochemical exploration. – 2003. – V. 77. – № 2–3. – P. 167–175.
  35. Minimalization of ash from Iranian Gilonite by Froth Flotation / R.J. Doodran, S. Khakmardan, A. Shirazi, A. Shirazy // Journal of Minerals and Materials Characterization and Engineering. – 2021. – V. 9. – P. 1–13.
  36. Shirazi A., Hezarkhani A., Shirazy A. Remote sensing studies for mapping of iron oxide regions, South of Kerman, Iran // International Journal of Science and Engineering Applications. – 2018. – V. 7. – № 4. – P. 45–51.
  37. Shirazi A., Shirazy A., Karami J. Remote sensing to identify copper alterations and promising regions, Sarbishe, South Khorasan, Iran // International Journal of Geology and Earth Sciences. – 2018. – V. 4. – № 2. – P. 36–52.
  38. Grunsky E., Agterberg F. Spatial and multivariate analysis of geochemical data from metavolcanic rocks in the Ben Nevis area, Ontario // Mathematical Geology. – 1988. – V. 20. – № 7. – P. 825–861.
  39. Cheng Q., Agterberg F., Ballantyne S. The separation of geochemical anomalies from background by fractal methods // Journal of Geochemical exploration. – 1994. – V. 51. – № 2. – P. 109–130.
  40. Mandelbrot B. How long is the coast of Britain? Statistical self-similarity and fractional dimension // Science. – 1967. – V. 3775. – № 156. – P. 636–638.
  41. Chen G., Cheng Q., Zhang H. Matched filtering method for separating magnetic anomaly using fractal model // Computers & Geosciences. – 2016. – V. 90. – P. 179–188.
  42. Unreliable determination of fractal characteristics using the capacity dimension and a new method for computing the information dimension / J. Liu, W. Ding, J. Dai, G. Zhao, Y. Sun, H. Yang // Chaos, Solitons & Fractals. – 2018. – V. 113. – P. 16–24.
  43. Graphical interactive generation of gravity and magnetic fields / A. Pignatelli, I. Nicolosi, R. Carluccio, M. Chiappini, R. von Frese // Computers & Geosciences. – 2011. – V. 37. – № 4. – P. 567–572.
  44. Mandelbrot B.B., Passoja D.E., Paullay A.J. Fractal character of fracture surfaces of metals // Nature. – 1984. – V. 308. – № 5961. – P. 721–722.
  45. Mandelbrot B.B. The fractal geometry of nature. – New York: WH freeman, 1982. – 460 p.
  46. Number-average size model for geological systems and its application in economic geology / Q.F. Wang, L. Wan, Y. Zhang, J. Zhao, H. Liu // Nonlinear Processes in Geophysics. – 2011. – V. 18. – № 4. – P. 447–454.

47. Zuo R., Xia Q., Zhang D. A comparison study of the C–A and S–A models with singularity analysis to identify geochemical anomalies in covered areas // *Applied Geochemistry*. – 2013. – V. 33. – P. 165–172.
48. Guan W., Hu H., Wang Z. Permeability inversion from low-frequency seismoelectric logs in fluid-saturated porous formations // *Geophysical Prospecting*. – 2013. – V. 61. – № 1. – P. 120–133.
49. Panichev A. Rare earth elements: review of medical and biological properties and their abundance in the rock materials and mineralized spring waters in the context of animal and human geophagia reasons evaluation // *Achievements in the Life Sciences*. – 2015. – V. 9. – № 2. – P. 95–103.
50. Ahmadi H., Rahmani A.B. Study on the mineral anomalies of Muqur-Chaman fault and its comparison with Harirud (Herat) fault (Afghanistan) using geophysical and remote sensing (Aster - HyMap) data // *Geology and bowels of the earth*. – 2018. – № 1 (66). – P. 28–38.
51. Agharezaei M., Hezarkhani A. Delineation of geochemical anomalies based on Cu by the boxplot as an exploratory data analysis (EDA) method and concentration-volume (CV) fractal modeling in Mesgaran mining area, Eastern Iran // *Open Journal of Geology*. – 2016. – V. 6. – № 10. – P. 1269–1278.
52. Daigle H., Johnson A., Thomas B. Determining fractal dimension from nuclear magnetic resonance data in rocks with internal magnetic field gradients // *Geophysics*. – 2014. – V. 79. – № 6. – P. 425–431.
53. Meakin P. Fractal aggregates in geophysics // *Reviews of Geophysics*. – 1991. – V. 29. – № 3. – P. 317–354.
54. Mazzarella A., Tranfaglia G. Fractal characterisation of geophysical measuring networks and its implication for an optimal location of additional stations: an application to a rain-gauge network // *Theoretical and Applied Climatology*. – 2000. – V. 65. – № 3. – P. 157–163.
55. Turcotte D.L. Fractals in geology and geophysics // *Pure and applied Geophysics*. – 1989. – V. 131. – № 1. – P. 171–196.
56. Ghorbani M. The economic geology of Iran: mineral deposits and natural resources. – New York: Springer, 2013. – 569 p.
57. Lehmann B. Economic geology of rare earth elements in 2014: a global perspective // *European Geologist*. – 2014. – V. 37. – P. 21–24.
58. Menard S. Applied logistic regression analysis. Sage publications. – London: Sage Publications, 2001. – 111 p.
59. Guan W., Hu H., Wang Z. Technospheric mining of rare earth elements from bauxite residue (Red Mud): process optimization, kinetic investigation, and microwave pretreatment // *Scientific Reports*. – 2017. – V. 7. – № 1. – P. 1–9.
60. Zhang W., Liao G., Qin Q. Based on open-source GIS platform to build 2D visual geophysical information management software // *Geophysical and Geochemical Exploration*. – 2014. – V. 5. – P. 1064–1069.
61. Faulds J.E. Geologic map and cross sections of the McGinness Hills Geothermal Area – GIS data. – Las Vegas, University of Nevada, 2013.
62. Pawlowski R. GIS applied to exploration: Caserta Block, Central Apennines, southern Italy // *The Leading Edge*. – 2000. – V. 19. – № 2. – P. 193–196.
63. Ekosse G., Fouche P.S. Using GIS to understand the environmental chemistry of manganese contaminated soils, Kgwakgwe area, Botswana // *Journal of Applied Sciences and Environmental Management*. – 2005. – V. 9. – № 2. – P. 37–42.
64. Prospecting for polymetallic mineralization using step-wise weight assessment ratio analysis (SWARA) and fractal modeling in Aghkand Area, NW Iran / S. Shahsavari, J.A. Rad, P. Afzal, N. Nezafati, A.M. Akhavan // *Arabian Journal of Geosciences*. – 2019. – V. 12. – № 7. – P. 1–10.
65. Yan Z.-H. Seismic random noise attenuation based on empirical mode decomposition of fractal dimension // *Chinese Journal of Geophysics*. – 2017. – V. 60. – № 7. – P. 2845–2857.
66. Al-Ghamdi A., Aguilera R., Clarkson C.R. Cementation exponent estimation for complex carbonate reservoirs using a triple porosity model // *Society of Petroleum Engineers - SPE/DGS Saudi Arabia Section Technical Symposium and Exhibition*. – Al-Khobar, Saudi Arabia, 2011. – P. 159–170.
67. Verifiable fuel cycle simulation model (VISION): a tool for analyzing nuclear fuel cycle futures / J.J. Jacobson, A.M. Yacout, G.E. Mathern, S.J. Piet, D.E. Shropshire, R.F. Jeffers, T. Schweitzer // *Nuclear Technology*. – 2010. – V. 172. – № 2. – P. 157–178.
68. MacLeod I.N., Jones K., Dai T.F. 3-D analytic signal in the interpretation of total magnetic field data at low magnetic latitudes // *Exploration geophysics*. – 1993. – V. 24. – № 3–4. – P. 679–688.
69. Geospace environment modeling 2008–2009 challenge: ground magnetic field perturbations / A. Pulkkinen, M. Kuznetsova, A. Ridley, J. Raeder, A. Vapirev, D. Weimer, R.S. Weigel, M. Wiltberger, G. Millward, L. Rastätter, M. Hesse, H.J. Singer, A. Chulaki // *Space Weather*. – 2011. – V. 9. – № 2. – P. 1–13.
70. Fogler M., Koulakov A., Shklovskii B. Ground state of a two-dimensional electron liquid in a weak magnetic field // *Physical Review B*. – 1996. – V. 54. – № 3. – P. 1853–1871.
71. Magnetic field induced lattice ground states from holography / Y.Y. Bu, J. Erdmenger, J.P. Shock, M. Strydom // *Journal of High Energy Physics*. – 2013. – V. 165. – P. 1–28.
72. N-electron ground state energies of a quantum dot in magnetic field / R.C. Ashoori, H.L. Stormer, J.S. Weiner, L.N. Pfeiffer, K.W. Baldwin, K.W. West // *Physical review letters*. – 1993. – V. 71. – № 4. – P. 613–616.
73. Gorbar E., Miransky V., Shovkovy I. Normal ground state of dense relativistic matter in a magnetic field // *Physical Review D*. – 2011. – V. 83. – № 8. – P. 1–26.
74. Depth estimation for magnetic/gravity anomaly using model correction / P. Liu, T. Liu, P. Zhu, Y. Yang, Q. Zhou, H. Zhang, G. Chen // *Pure & Applied Geophysics*. – 2017. – V. 174. – № 4. – P. 1729–1742.

Поступила: 24.09.2022 г.

Прошла рецензирование: 03.03.2023 г.

#### Информация об авторах

**Амин Карими Калварзи**, PhD, ассистент Технологического университета им. Амир Кабира (Тегеранский политехнический институт).

**Ареф Ширази**, PhD, ассистент Технологического университета им. Амир Кабира (Тегеранский политехнический институт).

**Адель Ширази**, PhD, ассистент Технологического университета им. Амир Кабира (Тегеранский политехнический институт).

**Амин Бейранванд Пур**, PhD, доцент Университета Малайзии Теренггану.

**Ардешир Хезархани**, PhD, профессор Технологического университета им. Амир Кабира (Тегеранский политехнический институт).

**Хамед Назерян**, ассистент Технологического университета им. Амир Кабира (Тегеранский политехнический институт).

**Тимкин Т.В.**, кандидат геолого-минералогических наук, доцент отделения геологии Инженерной школы природных ресурсов Национального исследовательского Томского политехнического университета.

**Ворошилов В.Г.**, доктор геолого-минералогических наук, профессор отделения геологии Инженерной школы природных ресурсов Национального исследовательского Томского политехнического университета.